Numerical Weather Prediction

Satellite Wind Superobbing

Forecasting Research Technical Report No. 451

Howard Berger (NWP SAF Visiting Scientist) and Mary Forsythe

email: nwp_publications@metoffice.com

©Crown Copyright

Satellite Wind Superobbing

Howard Berger[1] and Mary Forsythe[2]
(1) EUMETSAT NWP SAF Visiting Scientist/UW-CIMSS
(2) Met Office, Exeter UK

Abstract

Experiments have been performed to test the effect of superobbing atmospheric motion vectors within the Met Office's global numerical weather prediction model.In superobbing, the difference between observations and co-located backgrounds within a given three dimensional box are averaged to create one superobservation. Like data thinning, superobbing lowers the effect of the correlated error by reducing the data density. Superobbing, however, has the added advantage over data thinning of reducing the uncorrelated error through averaging.

The results of these experiments, as compared to a system similar to the Met Office's operational system using data thinning, have been neutral. The forecast impacts are slightly positive in the northern hemisphere while slightly negative in the tropics and southern hemisphere reflecting the differing effects of alternative observations in the different hemispheres. This minor impact suggests that random error might not be the predominate error within atmospheric motion vectors.

Introduction

In order to simplify the calculations and reduce the computing resources in most modern data assimilation systems, the observations and background fields used in these systems are assumed to have uncorrelated errors. This assumption, however, leads to potential problems with data types such as satellite winds for which correlated errors are significant. It has been suspected for some time that a sizeable component of the errors in the satellite wind observations are correlated in space and time, but it is only recently that an attempt has been made to test and quantify this idea. Bormann et al. (2002) carried out a collocation study of satellite wind – rawinsonde pairs and showed that if the sonde errors are assumed to be spatially uncorrelated, then the errors in satellite winds are significantly correlated for distances of up to 800 km. It is believed that this correlated error has limited the impact of satellite winds within most NWP models, particularly with the increasingly high resolution of the wind data.

Tests within the Met Office's global NWP system using new high-resolution satellite wind data sets at full resolution led to poorer analyses and forecasts than the lower resolution data sets that preceded them. It was thought that these results were related to the increased effect of correlated error in the high-resolution data. The correlated errors are currently overcome within the Met Office observation processing system by data thinning. Thinning the data to 800 km, the resolution to which Bormann et al.'s work showed significant correlation, is an extreme measure and would lead to substantial loss of data and detail in the wind field. Instead, the winds are thinned to a box size of 2 degrees (~200 km). This resolution reduces the influence of correlated errors but does not solve the

problem entirely. To further compensate for the error correlations, the observation errors for satellite winds were doubled from what was believed to be close to the true error in the observations, additionally reducing the impact of satellite winds on the analysis. The modification was shown to improve the forecast skill (Butterworth et al., 2002).

Although thinning and doubling the observation errors address the spatial correlation problem in a computationally inexpensive way, significant wind data are thrown away in the process. A possible alternative is to average the observations within a given box to create one observation that is positioned at the average location. Like thinning, this will reduce the number and resolution of the data input into the data assimilation system and should therefore reduce the problems resulting from spatially correlated error. A major concern of this method, however, is that it could lead to the loss of some meteorological features. Consider a simple example in the region of a jet. If winds above and below a jet core are averaged and the resulting wind placed at the average location, there is a danger that the slower wind will be positioned in the high speed region of the jet core, weakening the analyzed jet. But can this problem be avoided? In this paper, we propose an alternative: a superobbing scheme. Instead of averaging the observations, we will test a method to average the observation-background (O-B) or innovation. This method should allow us to use more of the wind data, potentially reducing the observation error, while reducing the risks of smoothing atmospheric features.

Theoretical Discussion:

Error Analysis and theory

Before the superobbing method can be implemented we must examine how superobbing would affect observation errors in the data assimilation system. Most data assimilation systems produce their analyses through a weighted average between a model first guess, or background, and observations. The extent to which the background and observations influence the analysis is determined by their respective assumed error values. Background errors are based on zonally and temporally averaged statistics from differences between 1- and 2-day forecasts valid at the same time for streamfunction, velocity potential, unbalanced pressure (ageostrophic pressure), and relative humidity. These background errors also contain a mass and wind constraint (Ingleby, 2000).

The observation errors are calculated by examining innovations: the difference between the observation and the background. This difference can be attributed both to the background error and to the observation error. Thus, if it is assumed that the background and observation errors are of similar magnitude, innovation statistics provide a measure of the upper limit of the observation errors. At the Met Office, the observation errors are calculated using a year's worth of innovation variances at different pressure levels. The variances are divided by two (to represent the split between observation and background error) and are then square-rooted so they can be expressed as a standard deviation. Superobbing, however, will change these observation errors by lowering the random error inherent in the satellite winds. In this section, we will derive an expression for a superob observation error to account for this effect.

Given a group of N observations (o_i) and corresponding background values (b_i) in a 3-dimensional box, a superob *s* can be formed as a weighted average of the observation minus the background. Namely:

$$s = b_o + \sum_i^N w_i (o_i - b_i) \tag{1}$$

where b_0 is the background value at the superob location and w_i is the weight for each o – b pair.

In matrix notation, this can be written:

$$s = b + W^T (O - B) \tag{2}$$

W,O and B are vectors of weights, observations and backgrounds respectively while s and b are the superob and background value at the superob location. The superob error, e_s is given by:

$$e_s = e_b + W^T (\varepsilon_o - \varepsilon_b) \tag{3}$$

e_b is the background error at the superob location, while ε_o and ε_b are error vectors within the superob box (relative to truth). Squaring and averaging the error in (3) over many boxes produces:

$$\overline{e_s e_s^T} = e_s^2 = e_b^2 + W^T \overline{(\varepsilon_o - \varepsilon_b) e_b} + \overline{e_b (\varepsilon_o - \varepsilon_b)^T} W + W^T \overline{(\varepsilon_o - \varepsilon_b)(\varepsilon_o - \varepsilon_b)^T} W \tag{4}$$

where $e_b^2 \equiv \overline{e_b e_b^T}$.

Assuming that over many boxes the observation and background errors are not correlated to each other ($\overline{\varepsilon_o \varepsilon_b^T} = \overline{\varepsilon_b \varepsilon_o^T} = \overline{e_b \varepsilon_o} = \overline{e_b \varepsilon_o^T} = 0$), equation (4) becomes:

$$e_s^2 = \overline{e_b^2} - W^T \overline{\varepsilon_b e_b} - \overline{\varepsilon_b^T e_b} W + W^T \underline{E} W + W^T \underline{B} W \tag{5}$$

where $\underline{E}$ and $\underline{B}$ are observation and background error covariance matrices ($\overline{\varepsilon_o \varepsilon_o^T}$) and ($\overline{\varepsilon_b \varepsilon_b^T}$) respectively. If we further assume that the background errors

are fully correlated with each other within a box, that all of the background errors within the box have the same magnitude, and that all of the innovations are weighted equally ($\frac{1}{N}$) then:

$$W^T \overline{\varepsilon_b e_b} = \overline{\varepsilon_b^T e_b} W = W^T \underline{B} W = \overline{e_b^2},$$

thus making:

$$\overline{e_b^2} - W^T \overline{\varepsilon_b e_b} - \overline{\varepsilon_b^T e_b} W + W^T \underline{B} W = 0.$$

Equation (5) is then

$$e_s^2 = W^T \underline{E} W \qquad (6)$$

Constant Observation Errors

If the observation errors (V_o, approximated as the innovation variance) are assumed to be constant, then (6) can be rewritten:

$$e_s^2 = V_o W^T \underline{C} W \qquad (7)$$

with $\underline{C}$ being a correlation matrix of the form:

$$\underline{C} = \begin{pmatrix} 1 & a & & a \\ a & & a & \\ & a & & \\ a & a & a & 1 \end{pmatrix}$$

and *a* being the average spatial correlation function over many boxes assumed to be constant on the length scales of a box.

Rewriting $\underline{C}$:

$$\underline{C} = (1-a)\underline{I} + a\underline{1_{mat}}$$

where $\underline{I}$ is the identity matrix and $\underline{1_{mat}}$ is a constant N x N matrix of value 1. Thus:

$$e_s^2 = V_o(1-a)(W^T \underline{I} W) + V_o a(W^T \underline{1_{mat}} W) \qquad (8)$$

We then define the uncorrelated observation error (V^u) ,the correlated error (V^c) and the weight vector W as:

$$V^u = V_o(1-a)$$
$$V^c = V_o a$$
$$W = \begin{bmatrix} \frac{1}{N} \\ \\ \frac{1}{N} \end{bmatrix}$$

The superob error simplifies to:

$$e_s^2 = \frac{V^u}{N} + V^C \tag{9}$$

By definition, for the individual observations:

$$V_o = V^u + V^c \tag{10}$$

Substituting into (9):

$$e_s^2 = V_o - (1-\frac{1}{N})V^u \tag{11}$$

Within a given box, the innovation variance is composed of four parts corresponding to the correlated background error, the correlated observation error, the uncorrelated background error and the uncorrelated observation error. The background error is assumed to be perfectly correlated (i.e. no uncorrelated part). The correlated component of the observation and background error are assumed to be constant within a box (perfect correlation) making those

associated innovation variances 0. From this assumption, the innovation variance within a box is only the uncorrelated part of the observation error. Namely:

$$V^{O-B} = V^{u} \tag{12}$$

This innovation variance can be treated as the population, of which a box makes up a sample. Thus, the population innovation variance can be estimated using the standard statistical formula:

$$V^{O-B} = \frac{N}{N-1} V_{box}^{O-B} \tag{13}$$

Substituting (12) and (13) into (11):

$$e_s^2 = V_o - V_{box}^{O-B} \tag{14}$$

Equation (14) gives a formula for calculating the new superob observation error based on the old observation error (V_o) and the innovation variance within a given box given that the observation errors within a box are constant.

Non-Uniform Observation Errors

If in equation (6), the observation errors are not constant then equation (14) is not valid. Instead, a more general expression must be used. Given that matrix $\underline{E}$ in (6) is symmetric and positive definite, (6) can be rewritten:

$$e_s^2 = W^T(\underline{D}\underline{C}\underline{D})W \tag{15a}$$

where $\underline{C}$ is the correlation matrix and W is the weighting vector described previously. $\underline{D}$ is a diagonal matrix of component observation errors within a box with the form:

$$D = \begin{pmatrix} \varepsilon_{oi} & 0 & 0 \\ 0 & & \\ & & 0 \\ 0 & 0 & \varepsilon_{on} \end{pmatrix}$$

where ε_{oi} represents the observation error of the *i*th component within the superob. Thus, (15a) can be expressed:

$$e_s^2 = \begin{bmatrix} \frac{1}{N} & \frac{1}{N} \end{bmatrix} \begin{pmatrix} \varepsilon_{oi} & 0 & & 0 \\ 0 & & & \\ & & & 0 \\ 0 & & 0 & \varepsilon_{on} \end{pmatrix} \begin{pmatrix} 1 & a & & a \\ a & & a & \\ & a & & \\ a & a & a & 1 \end{pmatrix} \begin{pmatrix} \varepsilon_{oi} & 0 & & 0 \\ 0 & & & \\ & & & 0 \\ 0 & & 0 & \varepsilon_{on} \end{pmatrix} \begin{bmatrix} \frac{1}{N} \\ \\ \frac{1}{N} \end{bmatrix} \quad \text{(15b)}$$

Using this formula to estimate the superob observation error, unlike the previous form, requires some knowledge of the observation error correlation (represented by *a*). With this knowledge, and the predefined observation errors, equation (15b) is a useful, general formula for estimating the superob observation error.

Discussion

Equations (14) and (15b) allow one to calculate in a simple way the superob observation error given many assumptions. Lorenc (1981) derives a superob and superob error formula using optimally chosen weights with the constraint of the background and superob errors being uncorrelated. Equations (14) and (15b), with the assumptions made to derive them, are a simplified form of Lorenc's formula and are not as optimal or general as Lorenc's method. Given our limited knowledge of the satellite winds' error characteristics, however, these simplified formulas do provide a reasonable estimate of the superob error. By examining these equations at their limits they are shown to be consistent with a conceptual understanding of errors.

Firstly, superobbing should not, in the limit of infinite observations, reduce the error to zero if any of the observations have correlated error. The superob reduces the random error within the superob, not the correlated error. This result can be shown in both formulas and becomes clear by looking at the perfectly correlated and perfectly uncorrelated cases.

Take for example, a box with wind innovations that are fully correlated (*a*=1 in equation 15). The difference between one observation with respect to its background is the same as the difference between any other observation and its background within the box. Hence, the value of one innovation would be identical to that of the others. A superob, the mean of the innovations, would be the same as any one of the component innovations, and the innovation variance in the box would be 0 since the innovations are identical. The error would be the average of component observation errors as shown in equation (14) (given that the average and the component observations are the same). An identical result can be derived from equation (15b). Winds with fully correlated errors have innovations with a variance of 0. The error would be the same regardless of the number of observations.

In the opposite extreme, superobbing a box of winds whose errors are fully uncorrelated (*a* = 0) would significantly reduce the error. If the correlated component in (9) was 0, it would follow that:

$$e_s^2 = \frac{V_{box}^o}{N-1} \qquad (16a)$$

where V_{box}^o is the innovation variance within a box. As N got very large, the superob error would be significantly reduced from the original observation error. To better compare with the non-uniform form, (16a) can be rewritten as:

$$e_s^2 = \frac{\sum_{i=1}^{N}\left[(O-B)_i - \overline{(O-B)}\right]^2}{N^2-N} \qquad (16b)$$

For non-uniform observation errors, setting *a*= 0 in (15b), the observation error

becomes:

$$e_s^2 = \frac{\sum_{i=1}^{N} \varepsilon_i^2}{N^2} \qquad (17)$$

an expression that is similar to (16b). The mean of the innovations in this uncorrelated case is relatively small compared to the correlated case while the variance is relatively large.

In reality, the observation error is partially correlated and partially uncorrelated, but these limits show us that the equations are consistent with a conceptual understanding of these errors. They also imply that winds with large correlated errors have a low innovation variance and a relatively large mean innovation while the innovations for highly uncorrelated errors have the opposite properties. It is useful to examine some of these statistics using real data, as is done in the next section.

Statistical Experiments

To examine how these statistics apply to real data, some simple calculations were performed on the Meteosat winds monitored for 8 October, 06 UTC 2003. First, outliers and wind vectors with a quality indicator (QI) of less than 60 (in a 0-100 scale) are removed from the data set. The QI is based on five vector tests and is described in detail in Holmlund et al. (2001) and Holmlund (1998). Then, the winds were binned in 2 degree by 100 hPa boxes, the same size as the thinning boxes described previously. In these boxes, the u and v O-B components are averaged to generate a superob u- and v-component O-B. The variance of the innovations in each box is also calculated.

As described previously, innovations within a box with a large variance and a small mean have highly uncorrelated errors. But, if the mean innovation within a box is high with a relatively small variance, then the correlated error dominates. To examine these errors in the wind data, it is instructive to plot the square of the mean innovation (the superob) versus the variance in each box. This plot is shown in

Figure 1 for a set of winds at 200 hPa. As seen in the figure, several of the boxes have a relatively high variance and a relatively low mean innovation. In these boxes superobbing will be most effective at reducing the observation error because the uncorrelated error dominates. Conversely, we would expect less benefit from superobbing the boxes with a large mean innovation and a small variance.

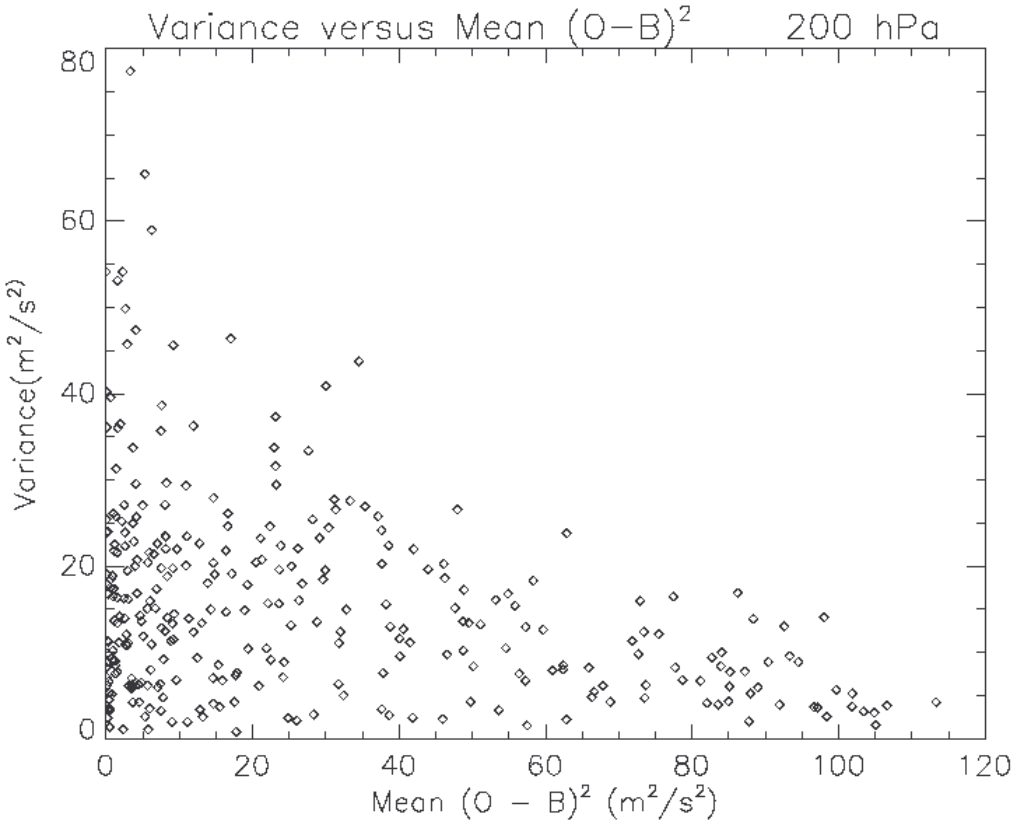

Figure 1: *Mean Squared Superob versus Variance. High variances and low mean (superob) values are regions where the winds have a large uncorrelated*

error. High mean values and low variances are regions where the winds have a large correlated error.

It is also useful to quantify the impact that superobbing will have on the observation errors. Equation (14) can be used to calculate the new superob observation error. Figure 2(a-d) shows a few statistics for the operationally assimilated winds from 1 January, 06 UTC, 2004. These winds were blacklisted as they are operationally including the QI thresholds as defined in Table 1. A superobbing box, as represented by the x-axis, represents an individual superobbing box comprised of one or more winds as shown in Figure 2c. Figure 2a shows the average assumed observation error for the winds in the box. These assumed errors are the observation errors used operationally within the data assimilation system. They are dependent on height and statistically determined from the standard deviation of a year's worth of innovations. Because the errors are only a function of height, this plot shows the bi-modal height distribution of the wind data set as the boxes with errors near 3 ms^{-1} are low level winds while the boxes with average errors near 6 ms^{-1} are in the upper levels. Figure 2b shows the resultant observation error based on equation (15b), while Figure 2d shows the percentage reduction of the original observation error. As seen in these figures, most of the observation errors are reduced from 10 to 40%, generally 1 to 2 metres per second. This reduction from (15b) approximates the amount of uncorrelated error removed through superobbing. The more accurately both correlated and uncorrelated errors are prescribed in the equation, the more accurately this formula represents the amount of uncorrelated error superobbing removes.

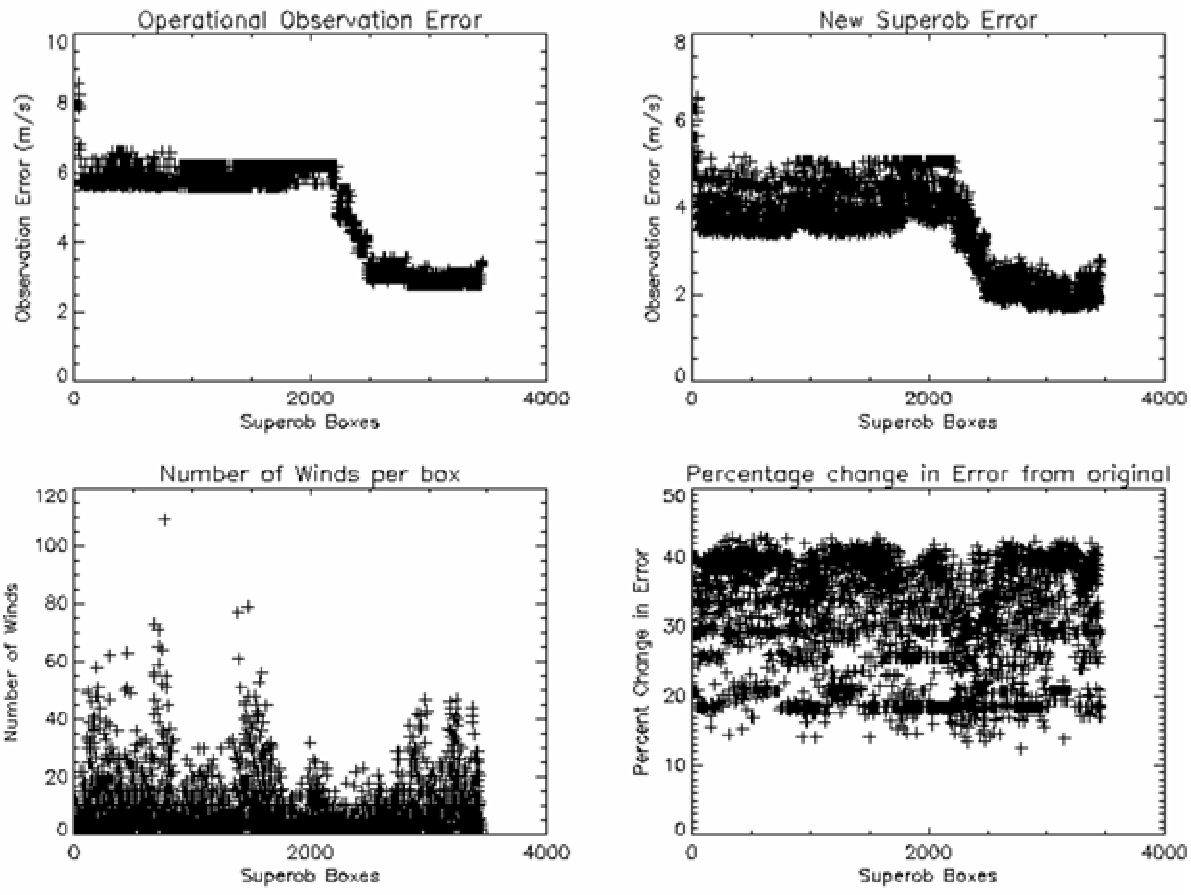

Figure 2*a.(Top left) Average operational observation error per box. b.(Top right) Reduced average observation error from superobbing. c.(Bottom Left) Number of Observations within superob boxes. d.(Bottom right) Percentage reduction of observation error due to superobbing*

Channel	Lat Band	Level	QI
IR	NH	High	85
IR	NH	Mid	80
IR	NH	Low	80
IR	TR	High	90
IR	TR	Mid	90
IR	TR	Low	90
IR	SH	High	85
IR	SH	Mid	80
IR	SH	Low	80
VIS	NH	High	**
VIS	NH	Mid	**
VIS	NH	Low	65
VIS	TR	High	**
VIS	TR	Mid	**
VIS	TR	Low	90
VIS	SH	High	**
VIS	SH	Mid	**
VIS	SH	Low	65
WV	NH	High	80
WV	NH	Mid	**
WV	NH	Low	**
WV	TR	High	90
WV	TR	Mid	**
WV	TR	Low	**
WV	SH	High	80
WV	SH	Mid	**
WV	SH	Low	**

Table 1 *Operational QI thresholds as a function of channel, latitude band and vertical level. ** represents combinations that are completely blacklisted.*

Forecast Impact Experiments

Experimental Design

To test the effect of superobbing on the model analyses and forecasts, a set of forecast impact experiments was run comparing forecasts and analyses of a control run without superobbing and a run with superobbing. The control run for these experiments is a low resolution (100 km) version of the Met Office's global NWP system with a forecast model described by Cullen et al. (1997) and a 3-dimensional variational assimilation system described by Lorenc et al. (2000).

In the control run all of the operational Met Office satellite data with the addition of the Binary Universal Form for the Representation of meteorological data (BUFR) GOES infra-red, water vapor and visible AMVs are assimilated. Currently, the Met Office operationally assimilates only the older SATOB format infra-red winds. The satellite winds in the control run are thinned to 2-degree 100 hPa boxes. The observation errors and quality indicator thresholds used at their operational values (see Table 1 for thresholds). The experimental setup is identical to the control run, except that the winds are superobbed in 2-degree/100 hPa boxes rather than thinned. The observation errors are reduced using equation (15b) taking a correlation value from Bormann et al. (2002). Different horizontal correlation values are used in the tropics and in the extra-tropics (0.26 and 0.35 respectively); otherwise, the correlation is constant.

The forecast impact experiments are run from 12z 24 January 2004, through 12z 17 February 2004. Four analyses and 6-hr forecasts are produced each day throughout the period along with one medium range forecast out to T+144-hours. All of the forecasts are verified on this medium range forecast initialized at 12z each day.

To conceptualize how much data is used in the thinning experiment versus the superobbing experiment, examine Table 2. The second column shows a typical number of available satellite winds (without quality control) for each experiment. The third column shows the typical number of winds that are assimilated (for thinning), and the total number of winds used as components for superobbing. The percentage of total winds is in parentheses. As the table shows, superobbing uses significantly more data. Keep in mind, however, that because the superobbing resolution is identical to thinning, the actual number of winds assimilated in the superobbing experiment (as superobs) is almost identical to the thinning experiment.

Experiment	Available Winds	Used winds (Percent total)
Control-Thinning	200,000	8000 (4%)
Superobbing	200,000	48,000 (24%)

Table 2: *Typical number of winds available and assimilated for a single run of the Control and Superob experiment. The majority of the increased number of winds for superobbing make up the components of the superob and are not assimilated directly.*

Results

The forecast impact of the superobbing experiments is small but generally negative. Figure 3 shows the root mean square (RMS) difference between the superob experiment and the control expressed as a percentage as compared to observations and analysis. In Figure 3, negative values show fields that have improved the forecast. Percentages with absolute values higher than 2% are considered significant. As can be seen from the plots the results are mixed and mostly small. We see significant negative impact for the 500 hPa 72-hour forecast (500 hPa) in the southern hemisphere and for the 96-hour forecast for

PMSL in the southern hemisphere when evaluated against observations. Conversely, we see fairly positive results of PMSL at T + 72 in the northern hemisphere against observations. Most of the fields, however, produce small impacts on either side of neutral. The results are also neutral against the analysis with one notable exception: 250 hPa winds in the tropics. The tropical winds will be investigated further in the next section. Otherwise some of the comparisons against analysis are better than those against observations and some are worse.

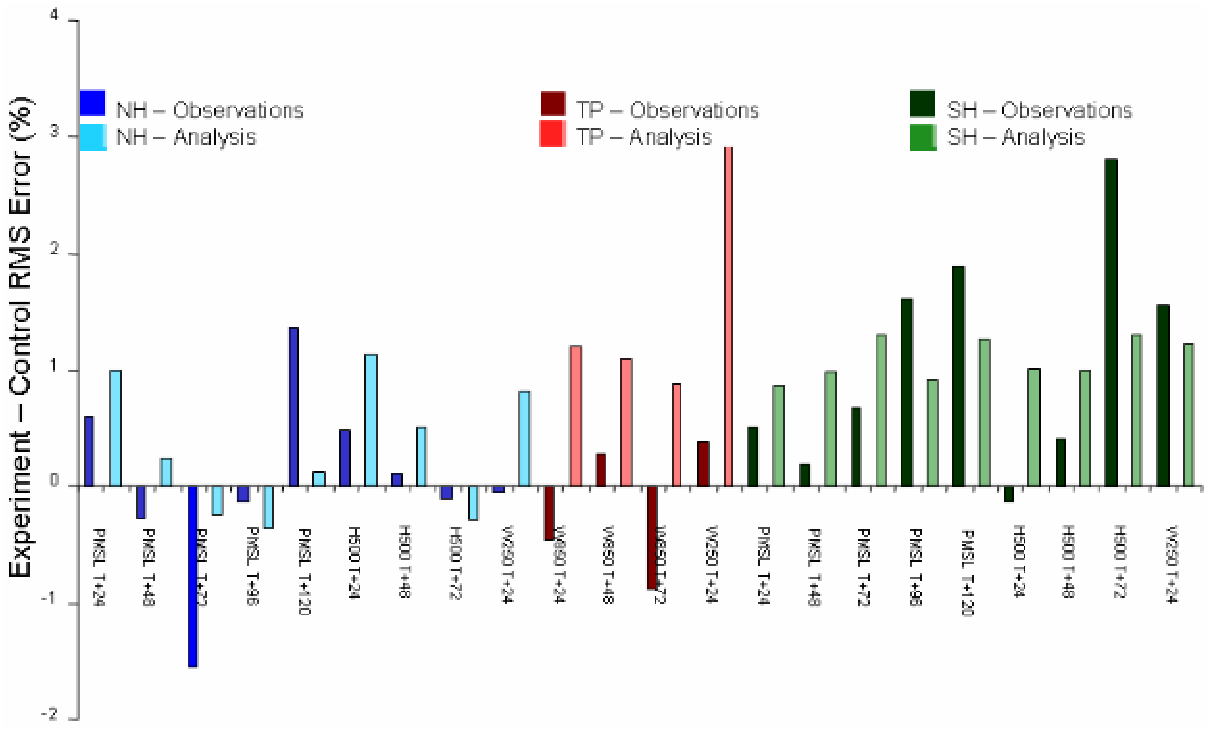

Figure 3: *Root Mean Squared differences between the experiment and the control for the northern hemisphere (NH), the tropics (TP) and the southern hemisphere (SH) for mean sea level pressure (PMSL), 500 hPa geopotential height (H500) and 250 and 850 hPa winds (W250 and W850 respectively) with respect to analysis and observations. Negative numbers show improvement of the experiment over the control.*

It is also instructive to examine how the forecast skill changes with time. Figure 4 shows the anomaly correlation of the model forecast of 500 hPa height as compared to its own analysis. From the plots, one can see that superobbing shows some skill (although probably not significant skill) against the analysis in the medium range for the northern hemisphere, but is generally negative for medium ranges in the tropics and the southern hemisphere. This result is consistent with the RMS in Figure 3.

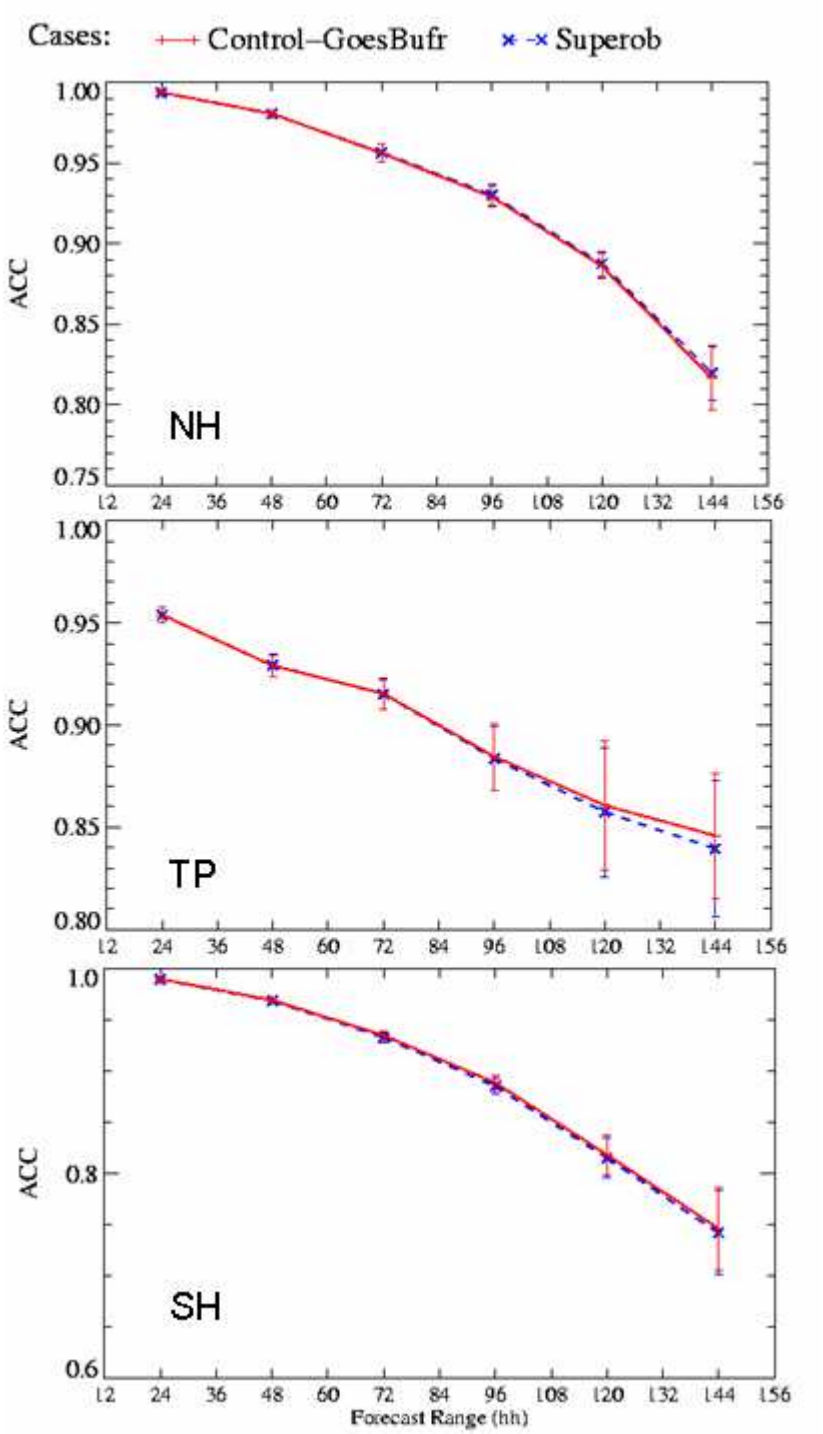

Figure 4*: 500 hPa anomaly correlations for the northern hemisphere (NH), tropics (TP), and southern hemisphere (SH) versus analysis. The solid red line represents the control run, while the dashed blue line represents the superob experiment. Superobbing shows positive results for long forecast times in the northern hemisphere, but is neutral or negative against the analysis in the southern hemisphere and the tropics.*

It is also worth examining how the forecasts vary from day to day throughout the trial. Figure 5 is a time series of 24 hour forecast differences between radiosondes and the model 250-hPa wind. The RMS vector error is plotted as a function of day. The daily 12z forecast for superobbing (blue dashed line) and the control (red solid line) is plotted for the northern hemisphere, the tropics and the southern hemisphere. The missing values are due to missing radiosonde data on the 10th. This problem does not affect the results shown.

Although the three regions shown in Figure 5 differ, all of them show both improved and degraded forecasts. The majority of the superob forecasts in the northern hemisphere are neutral or slightly positive as compared to the control. The forecasts on the 2nd and 3rd are consistently worse than the control in all three regions; The 12z forecast on the 4th is generally improved through superobbing. In general though, superobbing's effects are mixed and small at the 24 hour range. At longer ranges (not shown) the pattern continues with many mixed results, although they become slightly more extreme. The longer range is consistent with the 24 hour forecasts in that the northern hemisphere shows more forecast improvements than the southern hemisphere and the tropics.

Another important diagnostic tool for understanding the impact of a data type on the assimilation system is the analysis increment: defined as the difference between a model analysis and the model background, or first guess used to produce that analysis. Figure 6 shows the difference between the RMS of the analysis increments of the superobbing experiment and the control run for the 250 hPa u-component of the wind. A positive RMS difference implies that

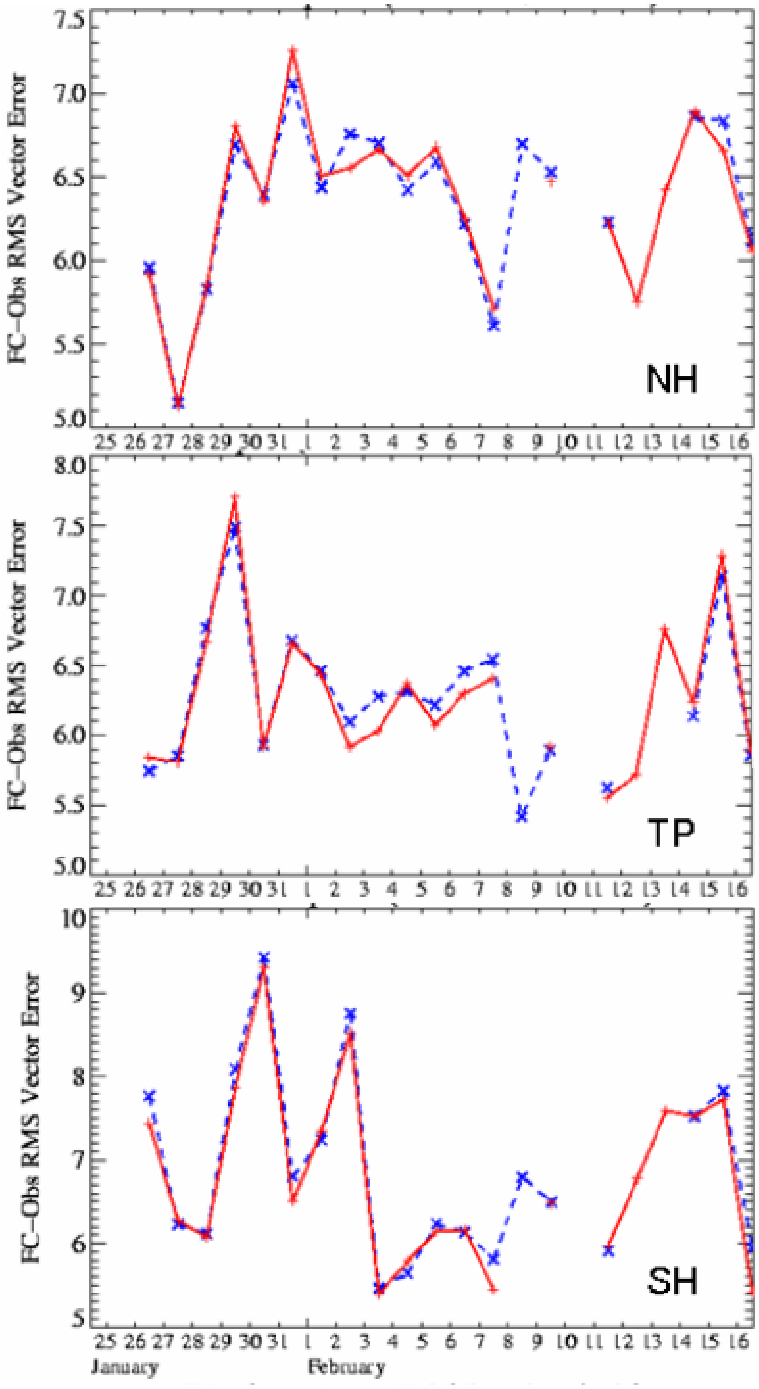

Figure 5*: 24-hour Forecast – Sonde RMS 250 hPa wind vector error time series for the Control run (red solid line) and the superob experiment (blue dashed) line. the forecasts are evaluated at 12z from 25 January, 2004 through 12z 17 February for the northern hemisphere (NH), tropics (TP) and southern hemisphere (SH). In all three regions superobbing both improves and degrades the control run, although the forecasts show the most improvement in the northern hemisphere.*

superobbing is, on the whole, changing the background more than the control run. A negative RMS would imply the opposite. As seen in the figure, the areas with positive RMS differences are spotty, but there are generally more positives than negatives.

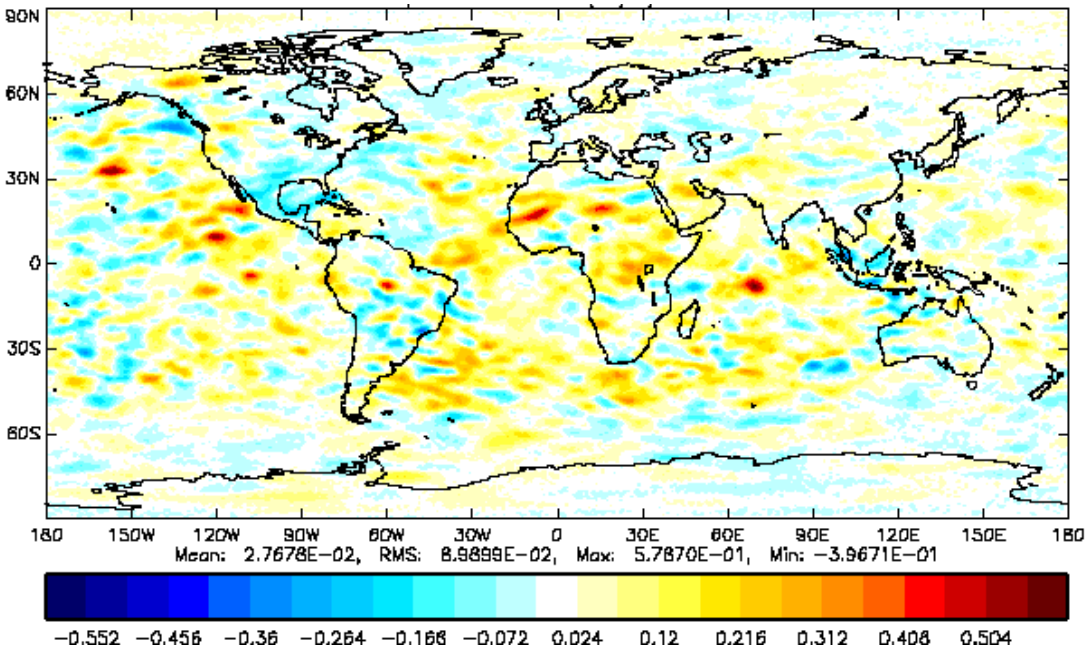

Figure 6: *Difference between the RMS of the superob trial and control run analysis increments. Positive values imply that superobbing is changing the background more than the control run.*

This result is not surprising. In our scheme, we are lowering the superob observation error, thus increasing the pull of the analysis toward observations. It is possible though, that superobbing is degrading the background used in the subsequent analysis so the winds must pull the background back to the observations. It is also possible that the increased number of winds influencing the analysis (see Table 2) has lead to the higher increments from superobbing. An additional explanation involves the fact that the control run selects the wind with the highest QI in a box. A model comparison is one of the QI tests, so a selected wind is likely to agree well with a model background, and is thus likely to make slightly less impact on the Met Office model then a superob.

Tropical Easterly Jet

It is useful to go beyond the statistics and investigate how superobbing affected a given forecast physically. Figure 7 shows the 24-hour forecast of 250 hPa u-component wind for the control (a) and the experiment (b). As shown, the superobbing experiment widens the maximum of the tropical easterly jet off the northwest coast of South America as compared to the control. The -14 ms $^{-1}$ contour extends over a slightly wider area than the control run. The -16 ms $^{-1}$ contour is more compact and slightly larger, however, for the control run. The -6 ms $^{-1}$ contour in the superobbing experiment also extends farther west and slightly farther to the north and south than in the control run.

Conversely, the subtropical jet centred at about 35S, 60W is slightly stronger from the control trial as compared to the superob. The geographic extent is fairly similar, but the jet in the control trial peaks at about 40 ms $^{-1}$ while the superob experiment peaks at 38 ms $^{-1}$.

Qualitatively comparing these two features to their analyses reinforces the mixed nature of these results. The geographic extent of the tropical easterly jet as shown in the analyses of both trials, (Figure 8a and b) matches the superobbing forecast better than the control forecast. The -6 ms^{-1} contour extends continuously west of 100W longitude in both analyses and the superob forecast, but is closed off in the control run forecast.

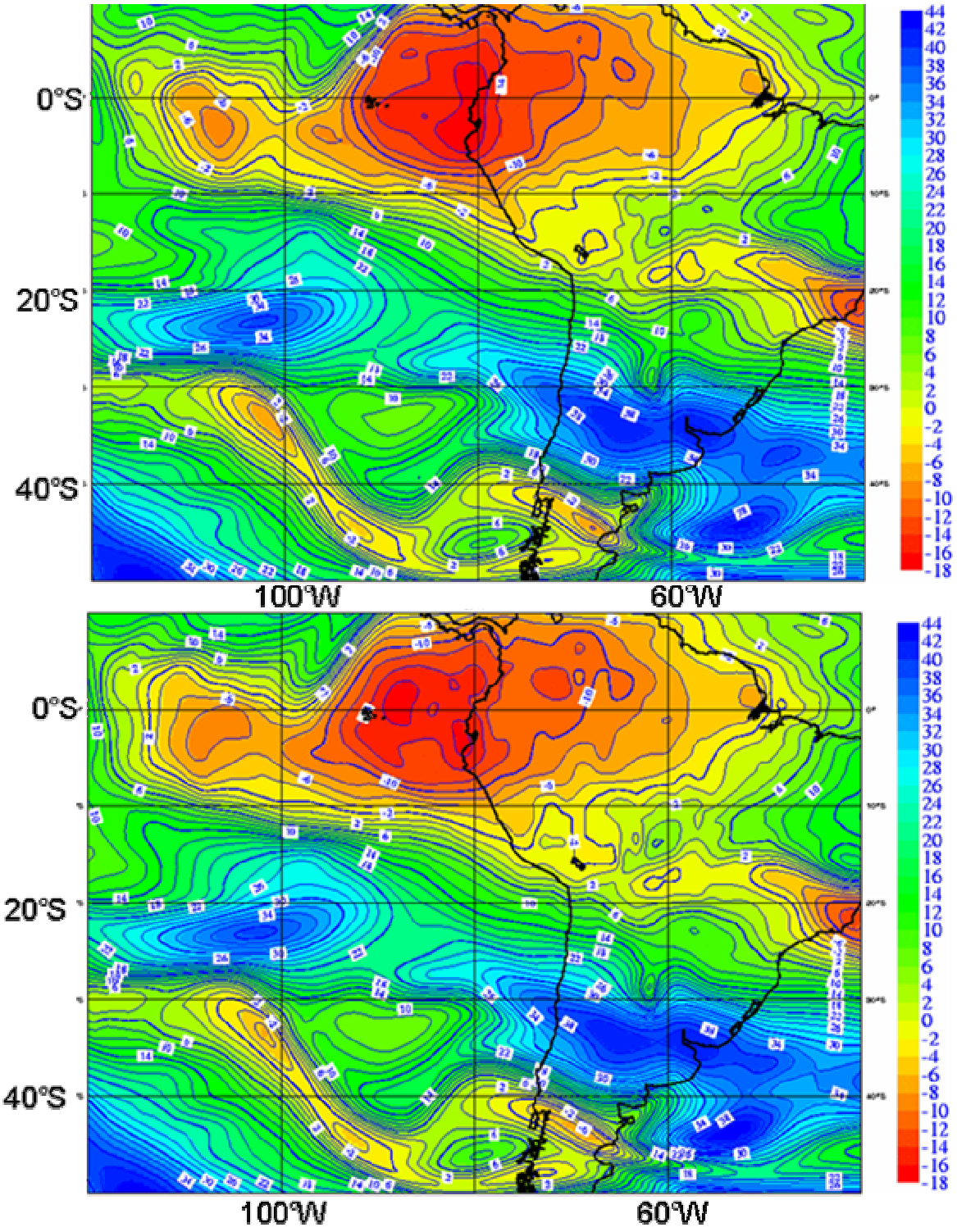

Figure 7: *24-hour forecast of the 250 hPa u-component wind(ms^{-1}) valid 12z 3 February 2004 for a. (top) control run and b.(bottom) superob experiment. The superobbing trial shows a stronger tropical easterly jet than the control but a slightly weaker subtropical jet over southern South America .*

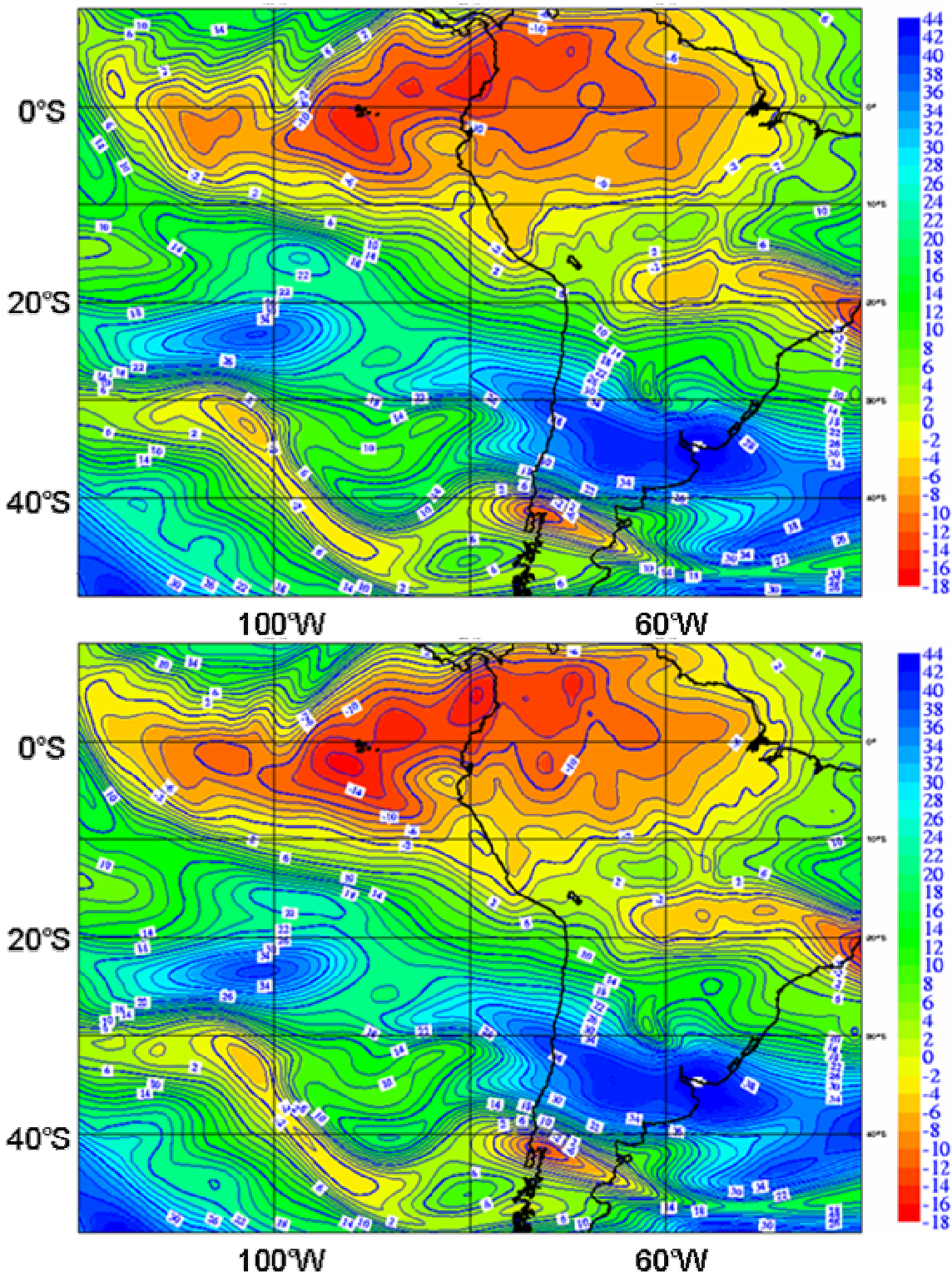

Figure 8: *Analysis of the 250 hPa u-component wind(ms^{-1}) valid 12z 3 February 2004 for a. (top) control run and b.(bottom) superob experiment. The analyses match the superobbing forecast better in the tropical easterly jet, but less well in the subtropical jet over southern South America.*

The analysis of the subtropical jet over southern South America, however, better matches the control forecast. Both analyses have a stronger subtropical jet than forecasted (greater than 44 ms^{-1}) with the peak value just east of 60 W. Although both forecasts have a good fix on the location of this maximum, the control run's maximum is slightly higher at approximately 42 ms^{-1} versus about 40 ms^{-1} in the superob trial.

As this discussion shows, even a qualitative and detailed examination of the model output shows the superobbing trial's mixed results. Superobbing seems to be capturing the tropical easterly jet better than the control run, but the control run has a slightly better handle on the subtropical jet. Over the mean in both trials (not shown) these features are represented with few differences. As with previous results, superobbing has a minor and mixed impact on forecast skill.

2.5-degree Experimental Results

Two experiments additional to the ones previously described were run to investigate the effects of thinning and superobbing at 2.5 degrees versus 2.0 degrees. Both had identical setups to the control and superob experiments, with the exception that one used a 2.5 degree thinning box (Control-2.5) and the other used a 2.5 degree superobbing box (Superob-2.5). Time series plots for the T + 24 250-hPa wind errors versus sondes are shown in Figure 9 for all four experiments. As seen in the plots, changing the box size did not make significant impact on the 24-hour forecasts. Some of the 2.5 degree forecasts were slightly better than the corresponding 2.0 degree forecasts and some were slightly worse. The results are more neutral in the northern and southern hemisphere

than in the tropics. The upper-level tropics are particularly sensitive to any changes in satellite winds, so this result is not surprising.

Examining the RMS differences between the 2.5 and 2.0 degree control runs (not shown) versus observations, shows that the percentages differed by more than 1 % for only three fields, and none of those differed by more than 1.3 %. The superob comparisons were even more similar as none of the fields differed by more than 1.0 %. More experiments are necessary to conclude that 2-degrees is the optimal resolution, but these experiments suggest that the forecasts are not very sensitive to small changes in box resolution.

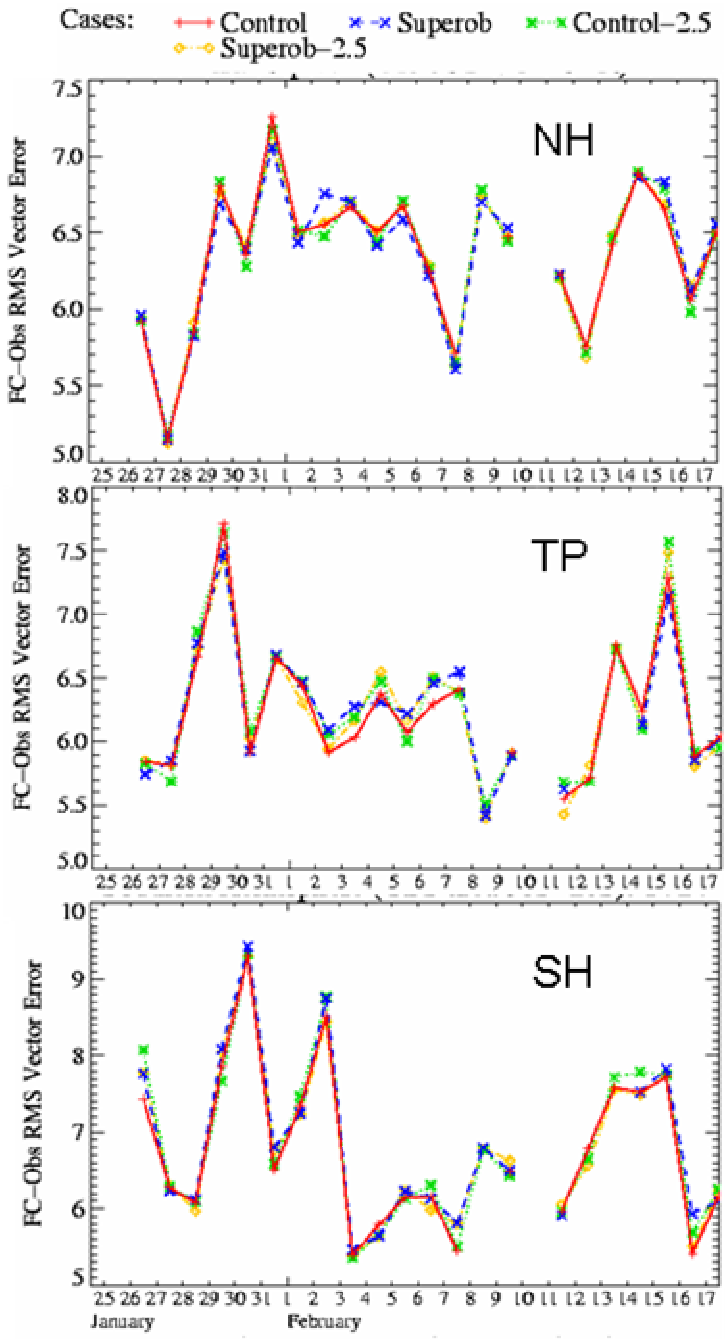

Figure 9*: 24-hour Forecast – Sonde RMS 250 hPa wind vector error time series for the Control run (red solid line), the superob experiment (blue dashed) line, the control with 2.5 degree thinning (green dots) and 2.5 degree superobbing (yellow diamond, dot/dash) The forecasts are evaluated at 12z from 25 January, 2004 through 12z 17 February for the northern hemisphere (NH), tropics (TP) and southern hemisphere (SH). Changing the box size does not change the forecast results significantly.*

Conclusions

As a whole, superobbing produced small analysis and forecast impacts as compared to its control. The impact was more positive in the northern hemisphere than in both the southern hemisphere and the tropics as compared to both observations and the corresponding analysis. A time series of individual forecasts also showed mixed results: some forecasts were positive, some negative, many were neutral. By examining a particular forecast in the upper-level tropical wind field, one could see some features that were captured better in the control, and some that were captured better in the superobbing experiment. Over the mean of the trial, however, these features were not represented very differently. Additionally, the two trials were not particularly sensitive to a small change in the thinning and superob box size.

A more difficult question to answer is why the results were so mixed. Theoretically, superobbing should remove some of the random error in the satellite wind data and should reduce the correlated error by the same amount as thinning. Many assumptions were made, however, to calculate the new superob observation errors. In particular, the correlation values used, although based on the values calculated by Bormann, are still assumed to be constant throughout a superob box. A deeper understanding of the correlated and random error of satellite winds is crucial to data assimilation and is an ongoing area of research. A more optimal error superobbing method like that suggested in Lorenc (1981), combined with increased understanding of the errors might improve the results as well.

It is also possible that we are not superobbing ideally. The choice of superobbing box size, both spatially and temporally, although shown to be

insensitive to a small change should be investigated more rigorously. Quality control is also of utmost importance, and it is possible that quality control can be optimized differently for superobbing and thinning.

Finally, the small impacts from superobbing suggest that the random error reduced by superobbing is not a primary source of error for AMVs. The height assignment and areas where clouds are not moving with the average wind are both sources of error and are probably more significant than the random component of error. Understanding all of these sources of error will lead to more positive impacts from AMVs in the future.

Acknowledgements

I'd like to thank the EUMETSAT NWP SAF VS scheme for its financial support as well as the Met Office for providing the facilities that made this work possible. Thanks also go to Chris Velden and the University of Wisconsin-CIMSS for providing my salary and for allowing me the opportunity to work at the Met Office. This funding was in part from NOAA Contract No.NA07EC0676. I'd like to personally thank Mary Forsythe who has worked with me at every step of this project from initial training to analyzing the results. John Eyre, Roger Saunders, Sean Healy, Bryan Conway and Chris Velden all provided valuable feedback and comments both on this manuscript and throughout my entire visiting scientist period. Thanks also go to Brett Candy and Steve English, particularly in helping me set up my assimilation experiments and interpreting the results.

References

Bormann, N., S. Saarinen, G. Kelly, J Thepaut (2002) The Spatial structure of observation errors in Atmospheric Motion Vectors from geostationary satellite data. EUMETSAT/ECMWF Fellowship Programme, Research Report No. 12, ECMWF, Reading,UK.

Butterworth, P, S English, F Hilton, K Whyte (2002) Improvements in forecasts at the Met Office through reduced weights for satellite winds, Met-Office, Bracknell, UK.

Cullen, M. J. P., T. Davies, M. H. Mawson, J. A. James, S. C. Coulter, and A. Malcolm, (1997). An overview of numerical methods for the next generation UK NWP and climate model. *Numerical Methods in Atmospheric and Ocean Modelling*, Lin, C. A., R. Laprise, and H. Ritchie, Eds., The Andre J. Robert Memorial Volume, 425-444.

Holmlund K, (1998) The utilization of statistical properties of satellite-derived atmospheric motion vectors to derive quality indicators. *Wea. Forecasting*, 13, 1093-1094

____, CS Velden, M Rohn (2001) Enhanced Quality Control Applied to High-Density Satellite-Derived Winds. *Mon. Wea. Rev., 129, 517-529*

Ingleby N.B (2000) The Statistical Structure of Forecast Errors and its Representation in the Met Office Global 3-Dimensional Variational Assimilation Scheme

Lorenc, A. C (1981) A Global Three-Dimensional Multivariate Statistical Interpolation Scheme. *Mon. Wea. Rev.,109,701-721*